Kasetsart J. (Nat. Sci.) 30 : 271-283 (1996)

Numerical Calculation of the Tidal Currents in Yashima Bay

Monton Anongponyoskun[1] and Takashi Sasaki[2]

ABSTRACT

A mathematical method was developed to predict the tidal motion in all study site. The basis of computation were the vertically integrated Navier-Stokes equations and continuity equation in an Eulerian system. The considered forces were inertia, coriolis, pressure gradient and friction. The effect of viscosity of sea water was introduced. The wind stress would be neglected. The solutions of tidal current computation were obtained on the basis of the scheme of explicit method by Ueno (1967). Since the solution of this model was solved by numerical method, so the effects of stability and convergence had to be considered. The use of the computational procedure was illustrated with results of tidal computations of the Yashima Bay, Japan.

Key words : Navier-Stokes equations, continuity equation, explicit method

INTRODUCTION

The numerical solution of the partial differential equations representing water motion would be considered since the solution of partial differential equations are difficult for estimating actual values. The effects of viscosity, inertia force, coriolis force, friction force and pressure were introduced.

The objected site was Yashima Bay. It was a shallow and small bay which was located at the eastern part of the Seto Inland sea, Takamatsu Prefecture, Japan as shown in Figure 1. The average depth of the bay over its total area was about 6.2 m. The maximum depth in the north part was about 14 m. The total area was about 6 km^2. There was main flow of sea water on the northtern. During ebb tide and flood tide the flow were eastward and westward, respectively. The residue of main flow was eastward. The average speed of main flow in each direction was about 1m/sec.

MATERIALS AND METHODS

1. Equation

For an incompressible fluid in which the density was a constant the continuity equation or mass conservation equation (Gerhard *et al.*, 1966; Lamb, 1932) was obtained as:

[1] Faculty of Fisheries, Kasetsart University, Bangkok 10900, Thailand.
[2] Faculty of Agriculture, Kagawa University, Japan.

$$\nabla \cdot V = 0$$

or

$$\frac{\partial u}{\partial x} + \frac{\partial v}{\partial y} + \frac{\partial w}{\partial z} = 0 \qquad (1)$$

2. Basic

The basic equations of motion, Navier-Stokes equations, were in the Eulerian form. The Cartesian axis x and y were taken clockwise in a horizontal plane of the undisturbed water surface, with the z axis vertically downward. The component of the velocities u, v and w were parallel to the coordinate axis x, y and z, respectively. The motion equations could be written in vector form as:

$$\frac{DV}{Dt} + 2\omega \times V = K - \frac{1}{\rho}\text{grad}P + \frac{1}{3}\nu\,\text{grad}(\text{div}V) + \nu\nabla^2 V \qquad (2)$$

where V = velocity of field in the xyz system

K = external force per unit volume

P = pressure at any point

ρ = density of fluid

ν = coefficient of kinematics viscosity

and $\nabla \cdot V$ = equation of continuity = 0

3. Time

In a turbulent motion let u, v and w be the velocity components which were composed of an average flow and random fluctuations are superimposed as:

$$u = \bar{u} + u', \qquad v = \bar{v} + v', \qquad w = \bar{w} + w' \qquad (3)$$

where $\bar{u}$, $\bar{v}$ and $\bar{w}$ = time average of velocities in the xyz coordinate

u', v' and w' = turbulent fluctuation velocities around the average state in the xyz coordinate by $\overline{u'}=0$, $\overline{v'}=0$ and $\overline{w'}=0$.

The time average of velocities at the fixed point in space were

$$\bar{u} = \lim_{T\to\infty}\frac{1}{T}\int_{-\frac{T}{2}+t}^{\frac{T}{2}+t} u\,dt, \quad \bar{v} = \lim_{T\to\infty}\frac{1}{T}\int_{-\frac{T}{2}+t}^{\frac{T}{2}+t} v\,dt, \quad \bar{w} = \lim_{T\to\infty}\frac{1}{T}\int_{-\frac{T}{2}+t}^{\frac{T}{2}+t} w\,dt \qquad (4)$$

4. Turbulence

In real water movement, it seemed that only turbulent stresses from horizontal velocity components were important. The molecular viscosity coefficient was small enough to be neglected when it was compared with eddy viscosity coefficients.

And then, following the assumptions that the coefficients of vertical (A_z) and horizontal (A_k) eddy viscosity coefficients were constant in the ocean. The equations of motion(Sasaki *et al.*, 1986) could be rewritten as:

$$\frac{D\bar{u}}{Dt} = -\frac{1}{\rho}\frac{\partial P}{\partial x} - 2\cdot\omega\cdot\bar{v}\cdot\sin\lambda + \frac{A_k}{\rho}\left[\frac{\partial^2\bar{u}}{\partial x^2} + \frac{\partial^2\bar{u}}{\partial y^2}\right] + \frac{A_z}{\rho}\left[\frac{\partial^2\bar{u}}{\partial z^2}\right]$$

$$\frac{D\bar{v}}{Dt} = -\frac{1}{\rho}\frac{\partial P}{\partial y} + 2\cdot\omega\cdot\bar{u}\cdot\sin\lambda + \frac{A_k}{\rho}\left[\frac{\partial^2\bar{v}}{\partial x^2} + \frac{\partial^2\bar{v}}{\partial y^2}\right] + \frac{A_z}{\rho}\left[\frac{\partial^2\bar{v}}{\partial z^2}\right]$$

$$\frac{D\bar{w}}{Dt} = -\frac{1}{\rho}\frac{\partial P}{\partial z} + g + \frac{A_k}{\rho}\left[\frac{\partial^2\bar{w}}{\partial x^2} + \frac{\partial^2\bar{w}}{\partial y^2}\right] + \frac{A_z}{\rho}\left[\frac{\partial^2\bar{w}}{\partial z^2}\right] \qquad (5)$$

where $2\omega\bar{u}\cos\lambda << g$

5. Boundary

In this model, boundary over bottom and sea surface weretreated. At the bottom $z = h(x,y)$ and sea surface $z = -\zeta(x,y,t)$.

Accordingly, the equation would be

$$u_h\frac{\partial h}{\partial x} + v_h\frac{\partial h}{\partial y} = w_h \qquad (6)$$

where u_h, v_h and w_h were velocities at the bottom in x, y and z direction, respectively.

Similar to sea surface $\zeta(x,y,t) = -z$

$$\frac{\partial\zeta}{\partial t} + u_{-\zeta}\frac{\partial\zeta}{\partial x} + v_{-\zeta}\frac{\partial\zeta}{\partial y} = -w_{-\zeta} \qquad (7)$$

where $u_{-\zeta}, v_{-\zeta}$ and $w_{-\zeta}$ were velocities at the sea surface in x, y and z direction, respectively.

Adding Eq.(6) to Eq.(7), therefore

$$w_h - w_{-\zeta} = \frac{\partial\zeta}{\partial t} + u_{-\zeta}\frac{\partial\zeta}{\partial x} + v_{-\zeta}\frac{\partial\zeta}{\partial y} + u_h\frac{\partial h}{\partial x} + v_h\frac{\partial h}{\partial y} \qquad (8)$$

6. Vertical

In this study, the vertical acceleration of the fluid particle was neglected because this acceleration was very small with respect to the acceleration of the gravity field. Also, the velocity of the water particle in the z direction could be neglected. Thus, all terms containing w in Eq.(5) were omitted.

The vertically averaged velocity components could be introduced according to

$$U = \frac{1}{h+\zeta}\int_{-\zeta}^{h}\bar{u}dz, \qquad V = \frac{1}{h+\zeta}\int_{-\zeta}^{h}\bar{v}dz \tag{9}$$

The distributions of the velocity components $\bar{u}$ and $\bar{v}$ over the vertical at a certain location could be expressed as a function of the vertically average velocity by introduction as:

$$\bar{u} = U + u_0, \qquad \bar{v} = V + v_0 \tag{10}$$

for these distributions, the following relations were defined:

$$\int_{-\zeta}^{h} u_0 dz = 0, \qquad \int_{-\zeta}^{h} v_0 dz = 0 \tag{11}$$

The discharges per unit width were defined as follows

$$M = \int_{-\zeta}^{h}\bar{u}dz = U(h+\zeta), \qquad N = \int_{-\zeta}^{h}\bar{v}dz = V(h+\zeta) \tag{12}$$

where M and N = discharges per unit width with respect to x and y directions, respectively.

Next, the continuity equation of turbulent flow was considered. By using the time average of velocity, the continuity equation might be rewritten as:

$$\frac{\partial\zeta}{\partial t} = -\left(\frac{\partial M}{\partial x} + \frac{\partial N}{\partial y}\right) \tag{13}$$

The motion equations in x and y direction might be rewritten when the frictional resistant values of Dronkers. (1964) at the bottom were introduced and wind stress was neglected as:

$$\frac{\partial M}{\partial T} = -\left(\frac{\gamma^2}{H}\sqrt{U^2+V^2} + 2\frac{\partial U}{\partial x} + \frac{\partial V}{\partial y} + \frac{U}{H}\frac{\partial H}{\partial x}\right)M$$

$$+\left(f - \frac{\partial U}{\partial y} - \frac{U}{H}\frac{\partial H}{\partial y}\right)N - gH\frac{\partial\zeta}{\partial x} \tag{14}$$

$$\frac{\partial N}{\partial T} = -\left(\frac{\gamma^2}{H}\sqrt{U^2+V^2} + 2\frac{\partial V}{\partial y} + \frac{\partial U}{\partial x} + \frac{V}{H}\frac{\partial H}{\partial y}\right)N$$

$$+\left(-f - \frac{\partial V}{\partial x} - \frac{V}{H}\frac{\partial H}{\partial x}\right)M - gH\frac{\partial\zeta}{\partial y} \tag{15}$$

in x and y direction, respectively.

7. Finite

The continuity Eq.(13) could be substituted by using central difference approximate as:

$$\zeta_{i,j}^{t+1} = \zeta_{i,j}^{t-1} - X_{i+1,j}^{t} + X_{i-1,j}^{t} - Y_{i,j+1}^{t} + Y_{i,j-1}^{t} \tag{16}$$

where $M \cdot \frac{\Delta t}{\Delta s} = H \cdot U \cdot \frac{\Delta t}{\Delta s} = X$

$$N \cdot \frac{\Delta t}{\Delta s} = H \cdot V \cdot \frac{\Delta t}{\Delta s} = Y$$

The equations of motion, Eq.(14) and Eq.(15)(Sasaki *et al.*, 1986), were rewritten into the finite differential forms in order to obtain X and Y in x and y direction respectively as:

$$X_{i,j}^{t+2} = (2A_{i,j}^{T} - 1) \cdot X_{i,j}^{t} + 2C_{i,j}^{T} \cdot Y_{i,j}^{t} + A_{i,j}^{T} \cdot R_{i,j}^{t+1} + C_{i,j}^{T} \cdot S_{i,j}^{t+1}$$

$$Y_{i,j}^{t+2} = (2B_{i,j}^{T} - 1) \cdot Y_{i,j}^{t} + 2D_{i,j}^{T} \cdot X_{i,j}^{t} + D_{i,j}^{T} \cdot R_{i,j}^{t+1} + B_{i,j}^{T} \cdot S_{i,j}^{t+1} \tag{17}$$

$$ZX_{i,j}^{t+1} = \zeta_{i+1,j}^{t+1} - \zeta_{i-1,j}^{t+1}$$

$$ZY_{i,j}^{t+1} = \zeta_{i,j+1}^{t+1} - \zeta_{i,j-1}^{t+1}$$

$$H_{i,j}^{t+1} = h_{i,j} + \frac{(\zeta_{i+1,j}^{t+1} + \zeta_{i-1,j}^{t+1} + \zeta_{i,j+1}^{t+1} + \zeta_{i,j-1}^{t+1})}{4}$$

$$UX_{i,j}^{T} = U_{i+1,j+1}^{T} - U_{i-1,j+1}^{T} + U_{i+1,j-1}^{T} - U_{i-1,j-1}^{T}$$

$$UY_{i,j}^{T} = U_{i+1,j+1}^{T} - U_{i+1,j-1}^{T} + U_{i-1,j+1}^{T} - U_{i-1,j-1}^{T}$$

$$VX_{i,j}^{T} = V_{i+1,j+1}^{T} - V_{i-1,j+1}^{T} + V_{i+1,j-1}^{T} - V_{i-1,j-1}^{T}$$

$$VY_{i,j}^{T} = V_{i+1,j+1}^{T} - V_{i+1,j-1}^{T} + V_{i-1,j+1}^{T} - V_{i-1,j-1}^{T}$$

$$HX_{i,j}^{T} = \frac{H_{i+1,j+1}^{T} - H_{i-1,j+1}^{T} + H_{i+1,j-1}^{T} - H_{i-1,j-1}^{T}}{H_{i,j}^{T}}$$

$$HY_{i,j}^{T} = \frac{H_{i+1,j+1}^{T} - H_{i+1,j-1}^{T} + H_{i-1,j+1}^{T} - H_{i-1,j-1}^{T}}{H_{i,j}^{T}}$$

$$A_{i,j}^{T} = (FT)_{i,j}^{T} - (2 \cdot UX_{i,j}^{T} + VY_{i,j}^{T} + U_{i,j}^{T} \cdot HX_{i,j}^{T}) \frac{\Delta t}{4\Delta s}$$

$$B_{i,j}^{T} = (FT)_{i,j}^{T} - (2 \cdot VY_{i,j}^{T} + UX_{i,j}^{T} + V_{i,j}^{T} \cdot HY_{i,j}^{T}) \frac{\Delta t}{4\Delta s}$$

$$C_{i,j}^{T} = f \cdot \frac{\Delta t}{2} - (UY_{i,j}^{T} - U_{i,j}^{T} \cdot HY_{i,j}^{T}) \frac{\Delta t}{4\Delta s}$$

$$D_{i,j}^{T} = -f \cdot \frac{\Delta t}{2} - (VX_{i,j}^{T} + V_{i,j}^{T} \cdot HX_{i,j}^{T}) \frac{\Delta t}{4\Delta s}$$

$$R_{i,j}^{t+1} = -g \cdot \frac{\Delta t^{2}}{\Delta s} (H_{i,j}^{t+1} \cdot ZX_{i,j}^{t+1})$$

$$S_{i,j}^{t+1} = -g \cdot \frac{\Delta t^{2}}{\Delta s} (H_{i,j}^{t+1} \cdot ZY_{i,j}^{t+1})$$

$$FT_{i,j}^{T} = 1 - \frac{\gamma^{2} \Delta t}{2} \cdot \frac{\sqrt{(U^{2})_{i,j}^{T} + (V^{2})_{i,j}^{T}}}{H_{i,j}^{T}}$$

$$U_{i,j}^{T} = X_{i,j}^{T} \cdot \frac{\Delta s}{\Delta t \cdot H_{i,j}^{T}}$$

$$V_{i,j}^{T} = Y_{i,j}^{T} \cdot \frac{\Delta s}{\Delta t \cdot H_{i,j}^{T}} \qquad (18)$$

The change of discharge in each interval time depended on changing of time (ΔT). Ueno(1967) expressed these terms into finite differential forms as:

$$X_{i,j}^{T+1} = (1 - \frac{8 \cdot A_{k} \cdot \Delta T}{\Delta s^{2}}) X_{i,j}^{T} + (\frac{2 \cdot A_{k} \cdot \Delta T}{\Delta s^{2}}) (X_{i+1,j-1}^{T} + X_{i-1,j-1}^{T} + X_{i+1,j+1}^{T} + X_{i-1,j+1}^{T})$$

$$Y_{i,j}^{T+1} = (1 - \frac{8 \cdot A_{k} \cdot \Delta T}{\Delta s^{2}}) Y_{i,j}^{T} + (\frac{2 \cdot A_{k} \cdot \Delta T}{\Delta s^{2}}) (Y_{i+1,j-1}^{T} + Y_{i-1,j-1}^{T} + Y_{i+1,j+1}^{T} + Y_{i-1,j+1}^{T}) \qquad (19)$$

8. Stability

The solutions of finite differential equation were not approximate in the sense of crude estimates. Finite difference methods generally gave solutions that were either as accurate as the data warrant or as accurate as was necessary for the technical purposes for which the solution were required.

In this study, for the accurate calculation the stability condition of steady flow was used in explicit scheme as related to the propagation velocity of sea water as:

$$\Delta t < \frac{\Delta s}{\sqrt{2 \cdot g \cdot h_{max}}} \qquad (20)$$

where Δs = grid interval

Δt = time step

h_{max} = maximum depth of sea area

g = acceleration due to gravity.

9. Initial conditions

The initial values of tidal level and tidal current at the starting time of calculation were equal to zero over the entire area of model as:

$$\zeta^0_{i,j} = 0, \quad X^0_{i,j} = Y^0_{i,j} = 0 \tag{21}$$

10. Tidal

In East part of Seto Inland sea, area of study, the tide was the simidiurnal tide. Then only two dominances of simidiurnal tide M_2 and S_2 were considered. The assumption of total amplitude of tide in this area was the sum of amplitude of constituents M_2 and S_2 for spring tide. Similar to the neap tide, the total amplitude of tide was 60% of $M_2 + S_2$.

Since only the simidiurnal tide had been considered, the initial phase of constituent M_2 was assumed in equal to initial phase of constituent S_2 in spring tide and neap tide.

The amplitudes and initial phases at boundary points were listed in Table 1. Prediction of tide height in a degree of accuracy could be made by the following equation.

$$\zeta^t_{i,j} = C_{i,j} \sin(\delta \cdot t + P_{i,j}). \tag{22}$$

where $C_{i,j}$ = amplitude of constituent

$P_{i,j}$ = initial phase of constituent

δ = frequency in degree per mean solar hour.

RESULTS AND DISCUSSION

This hydrodynamic model covered almost the Yashima Bay, Takamatsu prefecture, Japan. This model was also divided into many size grids as shown in Figure 2. The size of each grid was 100x100 m^2. The dimension was 59x99. The boundaries were located on the latitude 34° 21' N to 34° 25' N and longitude 134° 05' E to 134° 11' E. The parameters for using to find tidal current and tidal level of model during spring tide were shown in Table 1.

The tidal current computation programs had been written in FORTRAN language. They consisted of input, main and graphic programs. The input program was used to adjust and entry the data. The main program was used to calculate tidal level and tidal current of the model. The graphic program included many graphical and digital results.

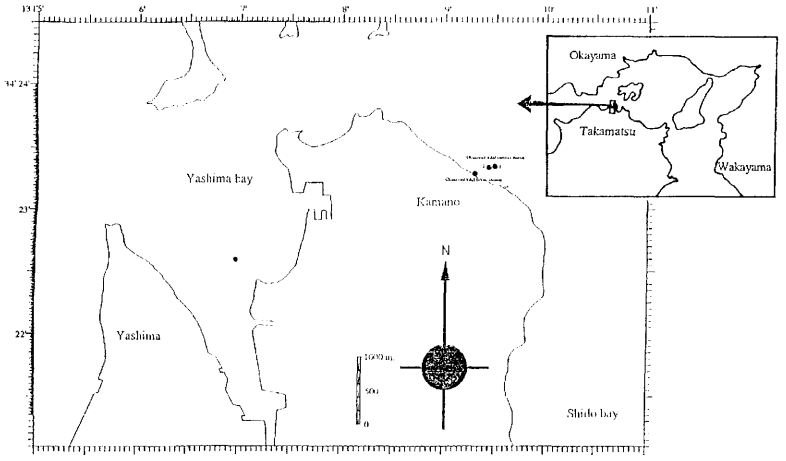

Figure 1 Surveying Station in Yashima bay and at Kamano, Kagawa Prefecture (1994).

Table 1 The parameters used to find tidal current and tidal level of model during spring tide.

Description	Unit	Symbol	Spring tide
Time step	second	Δt	10.0
Time interval	minute	ΔT	600.0
Grid interval	cm.	Δs	1.0×10^{4}
Angular rotation of earth	sec^{-1}	ω	7.893×10^{-5}
Angular speed of semidiurnal tide	degree/hour	δ	28.9841
Horizontal eddy viscosity coefficient	cm^2 / sec	A_k	2.0×10^{4}
Gravitational acceleration	cm / sec^2	g	980.0
Non-dimensional frictional constant		γ^2	0.0026
Mass density of sea water	g / cm^3	ρ	1.025
Hamonic amplitudes due to moon and sun at open boundary	cm	I	80.8
		J	78.8
		K	65.3
		L	60.6
Initial phases	degree	I	325.5
		J	328.0
		K	324.4
		L	334.0

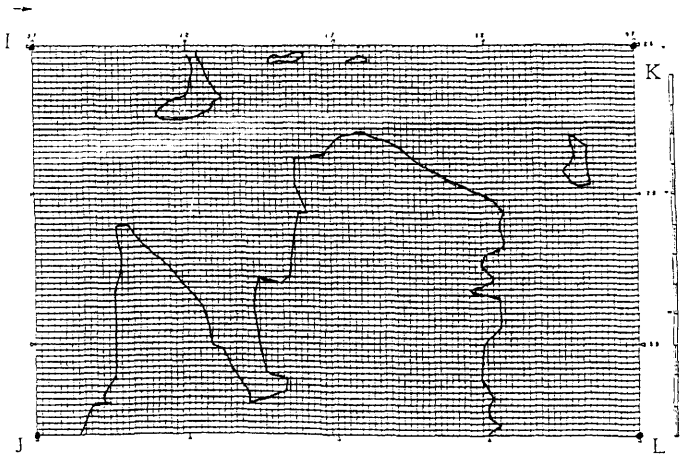

Figure 2 Modeling map.

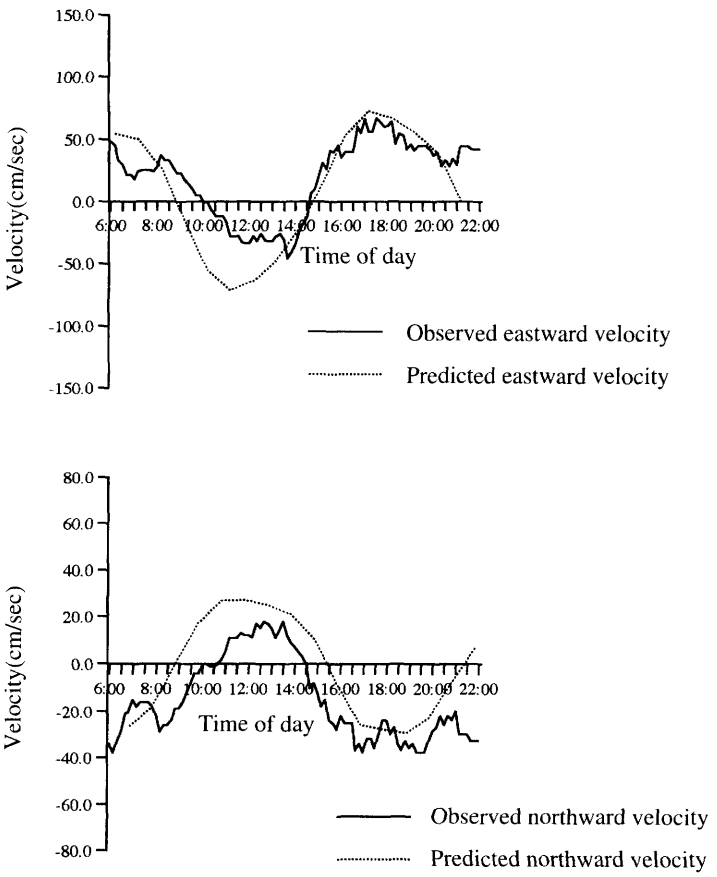

Figure 3 Comparison of tidal current during spring tide between predicted values at grid point (24,74) and observed values on 24 May, 1994 at Kamano Station 1.

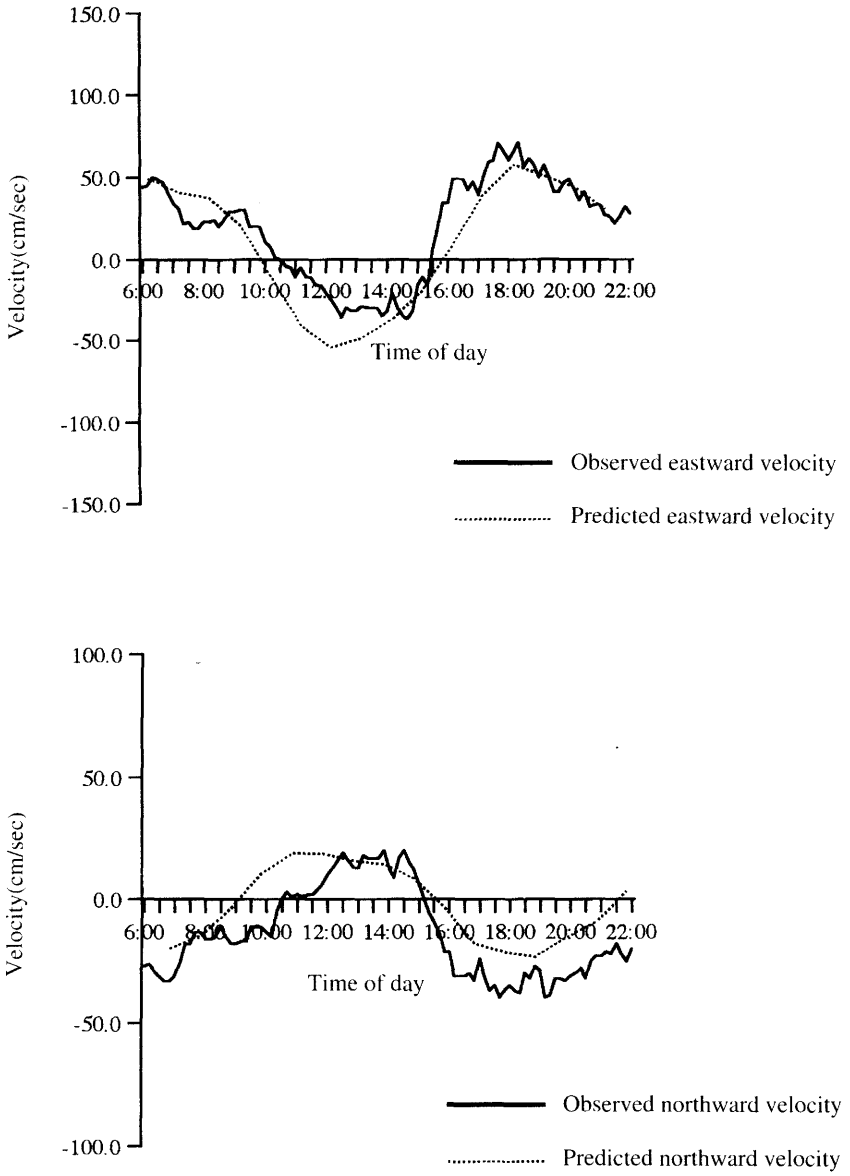

Figure 4 Comparison of predicted velocities at grid point (24,72) to observed velocities at Kamano Station 2 during spring tide on 24 May, 1994.

Comparisons of computed value with the actual observation values is necessary for checking the results of these predictions. The selected points for checking tidal current were in Kamano 2 points and in Yashima Bay one point and for checking the tidal level were in Kamano and in Yashima Bay. The stations for checking tidal current and tidal level were shown in Figure 1.

Checking tidal current, the comparisons of predicted velocity to observed velocity nearly the same place during spring tide were shown in Figure 3 to Figure 4. Checking tidal level, the comparisons of

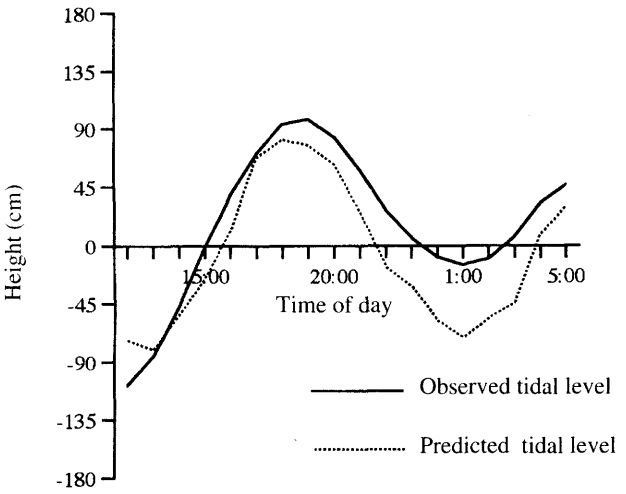

Figure 5 Comparison of tidal level during spring tide between prediction values at grid point (23,72) and observed values on 23 June , 1994 at Kamano station.

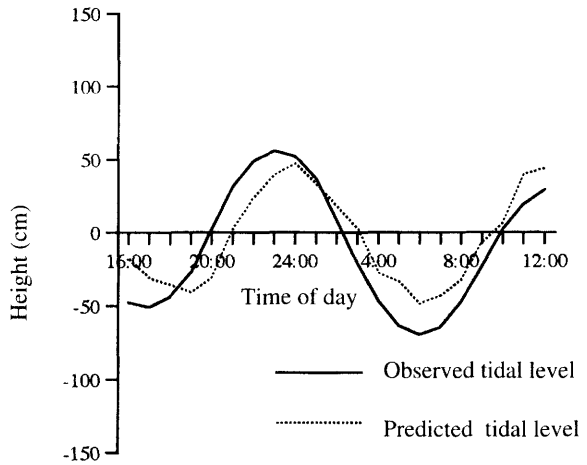

Figure 6 Comparison of tidal level during neap tide between prediction values at grid point (23,72) and observed values on 30 June , 1994 at Kamano station.

predicted height of sea water to observed height of sea water nearly the same place during spring tide and neap tide were shown in Figure 5 and Figure 6 respectively. From all comparisons, the results from prediction agreed with the results from observation. Therefore, we could rely on the magnitudes of velocities at all grid points of these models.

Figure 7 showed the distribution of maximum tidal stream during spring tide and neap tide which were obtained by the simulation of model. The direction and magnitude of arrows represented the direction and size of velocities. This model, during flood tide sea water was westward flow from eastern to western

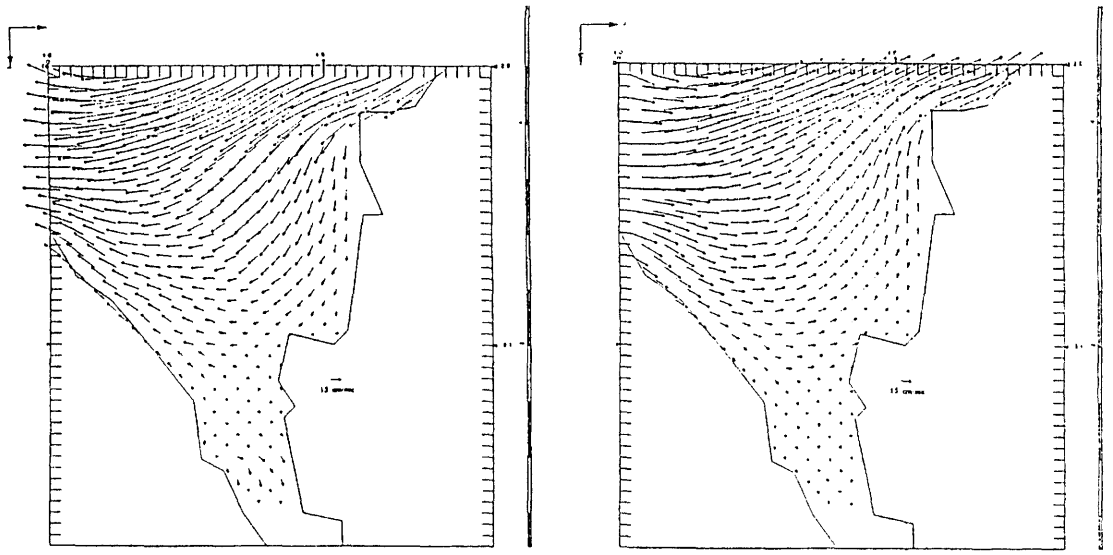

During flood tide at maximum stream. During ebb tide at maximum stream.

Destribution of tidal stream during spring tide.

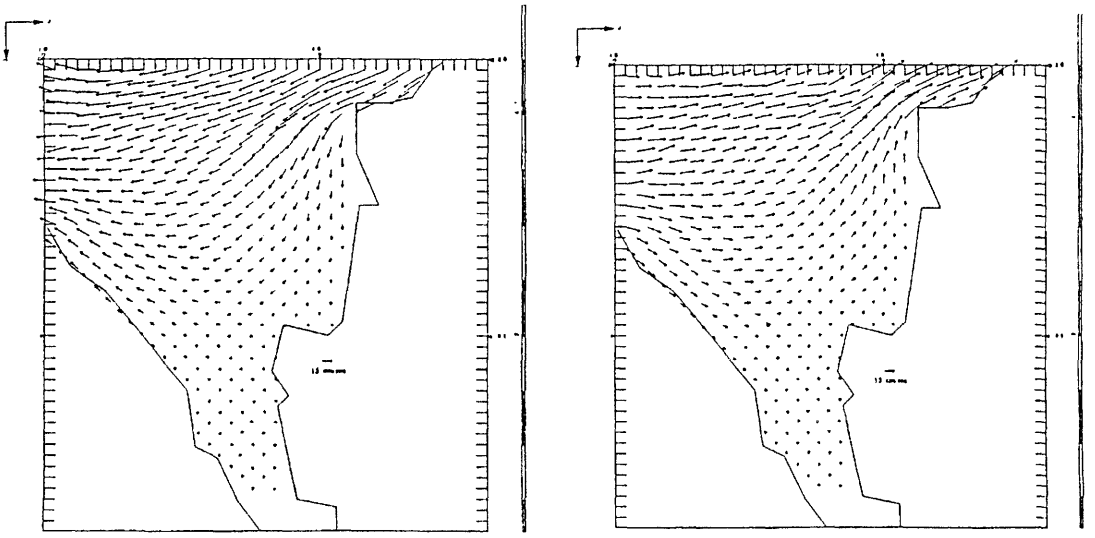

During flood tide at maximum stream. During ebb tide at maximum stream.

Destribution of tidal stream during neap tide.

Figure 7 Distributions of tidal stream during spring tide and neap tide in Yashima Bay.

and was eastward flow from western to eastern during ebb tide. The pattern of flow were continuous and smooth during flood tide and ebb tide. The fast velocities were in the main flow. The average velocity in the main flow was about 1 m/sec and in the Yashima Bay was about 0.3 m/sec. The patterns of flow during spring tide and during neap tide were the same. But during spring tide the magnitudes of velocity were greater than those during the neap tide.

CONCLUSION

In this study, numerical experiments were carried out on the basis of those current data. It was shown that the observed tidal currents were in agreement with the predicted values used on a two-dimensional numerical model. It confirm that the computed results obtained are those to be used sufficiently.

LITERATURE CITED

Dronkers, J.J. 1964. Tidal Computations in Rivers and Coastal Water. North-Holland Publishing Company. 502 p.

Gerhard, N., J. Willard, and Pierson, Jr. 1966. Principles of Physical Oceanography. Prentice-Hall, Inc. Engle Wood Cliffs, N.J. 545 p.

Lamb, H. 1932. Hydrodynamics, 6th ed. Cambridge University Press, Cambridge. 738 p.

Sasaki, T., T. Potapirom, and H. Inoue. 1986 a. Studies on the assessment of the allowable stocking capacity of yellowtail cultured in the Fukaura fish farm .Technical Bulletin of Faculty of Agriculture, Kagawa University. 37:131-148.

Sasaki, T., T. Potapirom, and H. Inoue. 1986 b. Studies on the assessment of the allowable stocking capacity of yellowtail cultured in the Fukaura fish farm.Technical Bulletin of Faculty of Agriculture, Kagawa University. 38:25-36.

Ueno, T. 1967. Numerical investigations of tides and surges near the bay of Osaka (part I). Bulletin of the Kobe Marine Observatory. 179:1-23